Pleistocene relief production in Laramide mountain ranges, western United States

Eric E. Small*
Robert S. Anderson
Department of Earth Sciences and Institute for Tectonics, University of California, Santa Cruz, California 95064

ABSTRACT

Gently sloped summits and ridges (collectively referred to as summit flats) are abundant in many Laramide ranges in the western United States. The erosion rate of summit flats is ~10 m/m.y., on the basis of the concentrations of cosmogenic radionuclides. Because erosion rates in valleys between summit flats are an order of magnitude faster, relief within these ranges is currently increasing by about 100 m/m.y. If summit-flat erosion is slower than rock uplift driven by the isostatic response to valley erosion, then this relief production could result in increased summit elevations. The mean depth of material eroded from a smooth surface fit to existing summit flats varies from 280 to 340 m in four Laramide ranges, based on geographic information system (GIS) analyses of digital elevation models. This erosion would result in a maximum of 250–300 m of rock uplift, assuming Airy isostasy. However, because the Laramide ranges examined here are narrow relative to the flexural wavelength of the lithosphere, erosionally driven rock uplift is limited to ~ 50–100 m. Over the past several million years, summit erosion would approximately offset this rock uplift. Therefore, we conclude that summit elevations have remained essentially constant even though several hundred meters of relief has been produced. On the basis of valley and summit erosion rates and the average depth of erosion, we estimate that relief production in Laramide ranges began at ca. 3 Ma. We hypothesize that this relief production was climatically driven and was associated with the onset or enhancement of alpine glaciation in these ranges.

INTRODUCTION

Changes in surface elevation reflect the combined effects of tectonics, erosion, and the isostatic response to erosion. For several reasons, it is important to quantify the portion of mountain summit and ridge elevation changes driven by the latter two processes. First, before elevation changes can be used to constrain tectonic processes in mountainous regions, the components of the elevation change driven by erosion and the isostatic response to erosion must be quantified (Small and Anderson, 1995; Abbott et al., 1997). Second, it is unknown whether tectonically driven uplift of the Himalayas and Western United States caused late Cenozoic global cooling (Ruddiman and Kutzbach, 1989; Raymo and Ruddiman, 1992) or whether global cooling produced geological evidence that has been misinterpreted as evidence for mountain uplift (England and Molnar, 1990; Molnar and England, 1990; Small and Anderson, 1995). Determining the magnitude of erosionally driven summit elevation change will help resolve this debate. Third, a positive feedback may exist between valley glacier erosion and rising summit and ridge elevations: increased elevations resulting from the isostatic adjustment to intense valley erosion could enhance the mass balance of glaciers, thereby increasing valley erosion and producing additional increases in elevation (Molnar and England, 1990). Although this hypothesized feedback is intriguing, it is unknown whether Pleistocene valley glacier erosion has actually led to increased summit elevations, or under what tectonic and geologic settings valley-glacier erosion may do so.

Rock uplift, vertical motions of rock relative to the geoid (England and Molnar, 1990), can be driven by either tectonic forcing or the isostatic response to erosion. In the absence of tectonic forcing (i.e., in tectonically "dead" ranges), changes in the mean elevation of a mountain range, $\Delta\hat{Z}$, equal the sum of the spatially averaged erosion, $\hat{E}$, and rock uplift driven by the flexural isostatic response to this mean erosional unloading, $U_{\hat{E}}(x,y)$:

$$\Delta\hat{Z} = \hat{E} + U_{\hat{E}}(x,y). \quad (1)$$

$\hat{E}$ is the product of the time-averaged mean erosion rate, $\dot{\hat{E}}$, over some time interval, t ($\hat{E} = \dot{\hat{E}}t$). $\Delta\hat{Z}$ is always negative for an eroding mountain range (no tectonically driven rock uplift) because the isostatic response to erosion is always less than erosion itself [$U_{\hat{E}}(x,y) < \hat{E}$]. Changes in elevation at a particular point in the landscape such as a mountain summit, ΔZ_S, equal the sum of erosion at that point, $E_S = \dot{E}_S t$, and rock uplift again driven by mean erosional unloading, $U_{\hat{E}}(x,y)$:

$$\Delta Z_S = E_S + U_{\hat{E}}(x,y). \quad (2)$$

In a tectonically inactive range, summit and ridge elevation changes must be negative when erosion is spatially uniform, $E_S = \hat{E}$. However, when erosion is spatially nonuniform, it is possible for changes in summit elevation to be positive, because local erosion may be less than rock uplift driven by the spatially averaged, or regional, erosion (Fig. 1). This situation is possible because the rigidity of the lithosphere horizontally distributes the isostatic response to erosion over a lengthscale of order ~10–100 km. For valley erosion to result in increased summit elevations, erosion of summits must be slower than the mean erosion rate, which requires that valleys must be growing deeper and/or wider.

Equation 2 can be used to calculate summit-elevation increases resulting from regional erosion over an interval of valley growth if (1) summit erosion is known; and (2) mean erosion can be constrained, from which the magnitude of $U_{\hat{E}}(x,y)$ can be estimated. In most mountain ranges, the amounts of summit and mean erosion that have occurred over some interval of valley growth cannot be measured, and only a maximum summit elevation increase over an unknown time interval can be estimated (e.g., Montgomery, 1994; and Gilchrist et al., 1994). Both summit erosion and mean erosion can be directly measured in only a

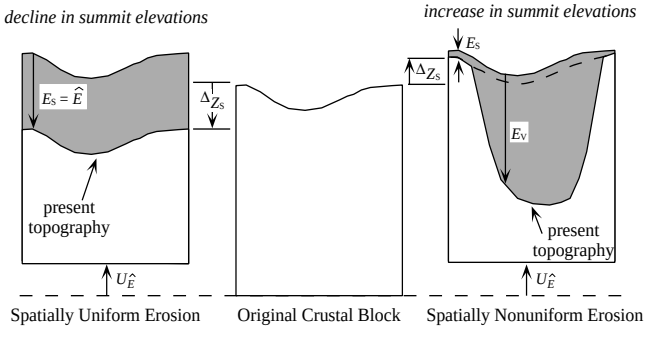

Figure 1. Two cases of mountain erosion. Center panel represents initial condition. When erosion (shaded area) is spatially uniform ($E_S = \hat{E}$), the sum of erosionally driven rock uplift ($U_{\hat{E}}$) and summit erosion (E_S) results in lower summit elevations (ΔZ_S) (left panel). When erosion is spatially variable (right panel), changes in summit elevation are positive because rock uplift is greater than summit erosion (eq. 2). Rock uplift is the same in each case because average erosion ($\hat{E}$), which drives rock uplift, is equal (shaded areas are the same size). The present geophysical relief ($\hat{R}$) is the mean elevation difference between a smooth surface connecting the highest points in the landscape (dashed line) and the current topography. It represents the average of valley erosion (E_V) minus summit erosion calculated at each point in the landscape, including summit flats.

*E-mail: esmall@earthsci.ucsc.edu.

few special settings. For example, in the Finisterre Range of Papua New Guinea, uneroded remnants of a sedimentary cover of known age exist on some summits and ridges (Abbott et al., 1997). At these sites, summit erosion since deposition of these rocks is zero. Furthermore, Abbott et al. (1997) estimated mean erosion as the average elevation difference between the present topography and a surface reconstructed from these summit remnants. On the basis of these values, and calculated values of the flexural rigidity, they estimated that ~300 m of erosionally driven rock uplift in the Finisterre Range has occurred over the past several million years.

In the absence of uneroded summit rocks, a reliable estimate of mean erosion can still be obtained if the rate of summit erosion is much slower than the mean rate of valley erosion, $\hat{\dot{E}}_V$, defined to be the spatially averaged lowering rate of all points within valleys. Assuming that the shape of the topography prior to valley growth can be reconstructed by fitting a smooth surface to present ridges and summits, the mean erosion required to create the present topography becomes

$$\hat{E} = \hat{R}\left[1 + \frac{E_S}{E_V - E_S}\right] \approx \hat{R} \text{ when } \dot{E}_S << \dot{E}_V, \quad (3)$$

We define "geophysical relief," $\hat{R}$, to be the mean elevation difference between two surfaces: a smooth surface connecting the highest points in the current landscape and the current topography itself (e.g., Abbott et al., 1997) (Fig. 1). It is different from "ordinary" relief, which is the elevation difference between valley bottoms and adjacent ridgetops. Geophysical relief represents the average erosion of all points within valleys minus the erosion that has lowered summits, over the time interval during which valleys have grown to their present size (Fig. 1). When $\dot{E}_S << \dot{E}_V$, $\hat{R}$ provides a good estimate of mean erosion, and thus can be used to calculate erosionally driven rock uplift over an interval of valley growth ($U_{\hat{R}}(x,y) \approx U_{\hat{E}}(x,y)$). We have chosen the modifier "geophysical" for this reason. The summit erosion that has occurred over this same interval can also be estimated from the present geophysical relief and summit and valley erosion rates:

$$E_S = \hat{R}\left[\frac{\hat{\dot{E}}_S}{\hat{\dot{E}}_V - \hat{\dot{E}}_S}\right]. \quad (4)$$

Substituting these quantities in equation 2, changes in summit elevation become

$$\Delta Z_S = \hat{R}\left(\frac{\dot{E}_S}{\dot{E}_V - \dot{E}_S}\right) + (U_{\hat{R}}(x,y). \quad (5)$$

When $\dot{E}_S = 0$, and tectonics are negligible, summit elevation changes are due primarily to erosionally driven rock uplift, which can be estimated from the existing topography (eq. 3). Here we calculate summit elevation changes in several Laramide ranges in the western United States, where summit erosion rates are so slow that this approach is valid.

STUDY AREA

Many western United States mountain ranges can be partitioned into two distinct geomorphic components: (1) deep valleys that have been intermittently glaciated during the Pleistocene; and (2) broad, nearly horizontal summits and ridges, which we will refer to collectively as summit flats. Previous summit flat research has been primarily descriptive, and many hypotheses have been proposed to explain their origin (reviewed by Madole et al., 1987). Summit flats, which are up to several square kilometers in area, are largely convex with low angle (typically 2°–3°) hillslopes. Regolith thickness is typically 1–2 m, the exceptions being tors several meters high, and bare-rock exposure at summit-flat edges. Hillslopes appear to be dominated by periglacial processes; sorted nets and stripes, felsenmeer, and nivation hollows are common.

We recognize no evidence of prior (wet-based) glaciation on summit flats. Glacial striations and erratic boulders are absent, and the bedrock-regolith interface of summit flats is much smoother than the bedrock surface of nearby glaciated troughs. In addition, there is no evidence of either past or modern fluvial channelization or landsliding. In the absence of glacial, fluvial, or landsliding processes, the transport of regolith, and the resulting lowering of summit-flat surfaces, proceeds only by periglacial creep. Because creep only transports unconsolidated material, summit-flat erosion is limited by regolith production and bare-rock weathering. On the basis of concentrations of produced in situ cosmogenic radionuclides (CRNs) (^{10}Be and ^{26}Al), we have calculated regolith production and bare-rock erosion rates from summit flats in the Wind River

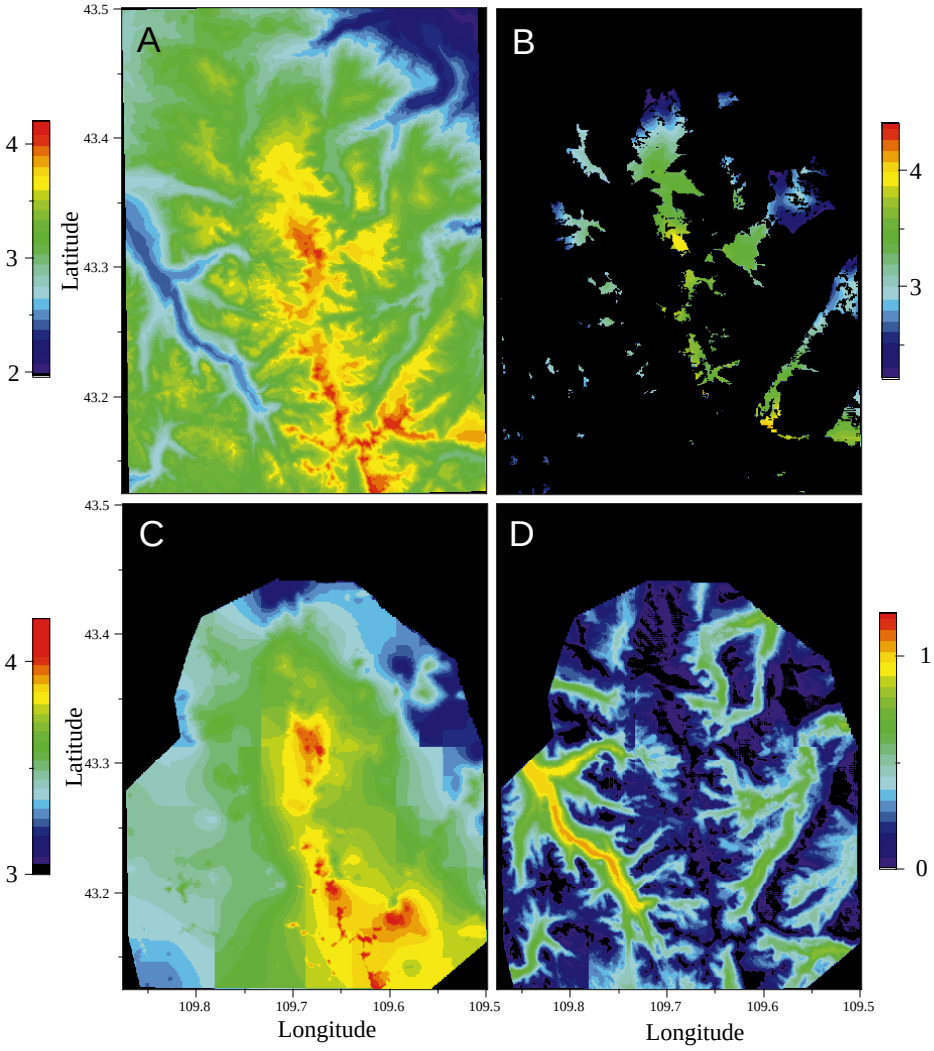

Figure 2. GIS analysis of geophysical relief in northern Wind River Range. Colors denote elevation in panels A–C and elevation difference in panel D (units are kilometers in all four). A: Topography of northern Wind River Range. B: Map of summit flats, constructed with a maximum slope threshold of 0.3 and minimum elevation threshold of 2.7 km. C: Smooth surface fit to summit flats in B. Discontinuities in surface result from partitioning of analysis region for computational reasons. D: Depth of erosion from surface fit to summit flats, determined by subtracting topography (A) at every point from the reconstructed surface (C).

(Wyoming), Beartooth (Wyoming and Montana), and Front Ranges (Colorado) (Small et al., 1997, 1998). Regolith production rates beneath ~1 m of regolith are about twice as fast as bare-rock erosion rates from tors and large boulders, ~15 and ~8 m/m.y., respectively. These values indicate that summit-flat erosion has been very slow over a 10^5 yr interval, the length of time over which CRNs have accumulated in the analyzed samples.

Previously reported denudation rates, $\hat{E}_D$, from the mountain ranges examined here are an order of magnitude faster than the summit-flat erosion rates we have calculated. Denudation rates, based on physical and chemical sediment balances, from mountain ranges with relief similar to those examined here are typically 100–150 m/m.y. (Ahnert, 1970). For example, the denudation rate in the northern Wind River Range is ~115 m/m.y. and that in the western Front Range and surrounding area is ~100 m/m.y. (Ahnert, 1970). These basin-averaged denudation rates likely reflect the intermittent alpine glaciation of the valleys. Denudation rates measured from glaciated basins similar in area (~100 km^2) to those examined here vary from ~100 to greater than 1000 m/m.y. (Hallet et al., 1996). Because summit flats represent only a small (10%) fraction, f_S, of the landscape, valley erosion rates are slightly faster than these landscape-averaged denudation rates:

$$\hat{E}_V = \hat{E}_D \left(\frac{1 - \left(\hat{E}_S / \hat{E}_D \right) f_S}{1 - f_S} \right). \quad (6)$$

Because the mean rate of valley erosion is ≥100 m/m.y. and the rate of summit flat erosion is ~10 m/m.y., geophysical relief within these ranges is currently increasing by roughly 100 m/m.y. If this valley growth has persisted for some time, it is possible that summit elevations are increasing as a result of valley erosion. Because summit erosion is nearly zero and is much slower than valley erosion ($\hat{E}_V >> \hat{E}_S \approx 0$), we can use equation 5 to estimate changes in summit elevation. This procedure requires measuring the mean elevation difference between a smooth surface fit to summits and the existing topography, $\hat{R}$.

TOPOGRAPHIC ANALYSIS

We used 30 m digital elevation models (DEMs) and a geographic information system (GIS) to determine $\hat{R}$ for the three ranges in which we measured regolith production and erosion rates, as well as the Uinta Range (Utah). This approach is illustrated with our analysis of the Wind River Range (Fig. 2). First, we generated summit-flat maps by selecting areas that had gentle slopes, high elevations, and no evidence for fluvial incision or glacial erosion. The use of a maximum slope threshold of 0.3 was based on slope distribution from summit flats visited in the field. Minimum elevation thresholds were low enough to include all summits and ridgetops within Pleistocene glaciated areas. Maps of low-sloped, high-elevation regions included some cirques and valley bottoms, which we removed from summit-flat maps (digitized by hand), based on morphology shown on 1:24 000 U.S. Geological Survey topographic maps. Summit flats represent ~10% of the Pleistocene glaciated region in each mountain range (Fig. 2B).

Second, we fit a smooth surface to summit-flat maps by using a regularized spline-with-tension technique (Mitasova and Mitas, 1993) (Fig. 2C). The largest elevation difference between the fitted surface and summit flats was ~20 m; the mean offset is close to 0 m. At the crest of each range, steep-sloped peaks at higher elevations than summit flats were added to the final fitted surface. The elevation and morphology of the final fitted surface are quite insensitive to both the slope and elevation thresholds used to generate the summit-flat maps and to the parameters used in the surface fitting procedure.

Finally, we constructed maps of the depth of erosion from beneath the surface fit to summit flats, $R(x,y)$, by subtracting off the original DEM topography (Fig. 2D). The depth of erosion varies from 0 m over summit flats to >800 m in the deepest valleys. In all four ranges, the distribution of $R(x,y)$ is bimodal: $R(x,y)$ for summit flats is near zero, and the second mode of ~300 m represents the most common depth of erosion beneath the reconstructed surface. The geophysical relief (i.e., the spatially averaged depth of erosion from the reconstructed surface), $\hat{R}$, is remarkably similar between the four ranges analyzed, varying from 280 m in the Uinta Range to 340 m in the Beartooth Range (Table 1).

TABLE 1. EROSION AND ROCK UPLIFT FOR FOUR MOUNTAIN RANGES IN THE WESTERN UNITED STATES

Mountain range	Geophysical relief, $\hat{R}$ (m)	Rock uplift (m) (no flexure)	Rock uplift (m) (flexure)	Summit erosion (m)	Summit-elevation change (m)
Wind River	295	250	70	45	25
Beartooth	340	290	90	55	35
Front Range	290	245	40	45	-5
Uinta	280	240	55	45	10

Note: Rock uplift with no flexure (Airy isostatic compensation) based on $\hat{R}$, ρ_c = 2700 kg/m^3. Flexurally modified rock uplift represents maximum uplift along range cross-section, calculated with elastic thickness h = 16 km (see Figure 4). Summit elevation change is the sum of flexurally modified rock uplift and surface lowering by summit erosion (eq. 5). All values are rounded to the nearest five meters.

CHANGES IN SUMMIT ELEVATIONS

The maximum response to surface-mass removal is the Airy isostatic response, set solely by the crust-mantle density contrast, ($U_{\hat{R}}(x,y) = \hat{R}(\rho_C/\rho_M)$ (Turcotte and Schubert, 1982). For the ranges considered, this varies between ~240 and ~290 m (Table 1). However, the finite rigidity of the lithosphere horizontally distributes the isostatic response to erosion, which should both decrease the expected rock uplift of the range crest and affect the adjacent basin edges. Given the range-parallel symmetry of these long, narrow ranges, we use a one-dimensional flexural model (Hetenyi, 1946) to calculate the effects of lithospheric rigidity on the uplift pattern. For the spatial pattern of erosional unloading (Fig. 3) to be used in the flexural calculation, we average the erosion parallel to each range crest, thereby assuming that this unloading extends infinitely along the range axis. On the basis of gravity modeling, Hall and Chase (1989) estimated a minimum effective elastic thickness of 16 km in the Wind River Range. We use this value for all four ranges. Both this minimum estimate of elastic thickness and the assumption that erosion extends infinitely along each range axis produce maximum estimates of the resulting rock uplift. The flexurally modified rock uplift is much less than the simple Airy isostatic response to erosion, even with the low elastic thickness value used (Fig. 3). Maximum erosionally driven rock uplift, which would occur near each range crest, varies from ~40 m in the Front Range to ~90 m in the Beartooth Range (Table 1).

In order to calculate summit-elevation changes driven by this rock uplift (eq. 2), we also must assess summit erosion, E_S. We estimate summit erosion (eq. 4) to be ~50 m in each range (Table 1),

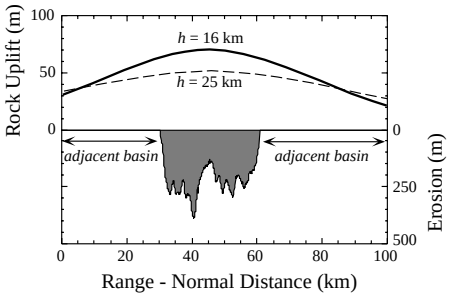

Figure 3. Erosion and resulting rock uplift for Wind River Range. Bottom: Erosion from surface fit to summit flats (from Fig. 2D) averaged parallel to range axis (shaded region). Maximum erosion exists roughly halfway between range crest (x = ~47 km) and margin of glaciated region. Top: Flexurally modified rock uplift resulting from erosion in bottom panel, for effective elastic thicknesses of 16 (solid) and 25 km (dashed). Erosionally driven rock uplift extends well beyond margin of glaciated region, into the adjacent basins.

based on the assumption that the time-averaged erosion rate is 15 m/m.y. and the rate of geophysical relief production ($\hat{E}_V - \hat{E}_S$) is 100 m/m.y. in each range. Although the calculations of erosionally driven rock uplift are reliable (they depend only on $\hat{R}$ and on the choice of flexural rigidity), these estimates of summit erosion are not as well constrained. For example, a doubling of the least well known quantity in equation 4, $\dot{E}_V$ (to 200 m/m.y.) would reduce summit erosion by roughly 50%. This uncertainty translates into only small absolute errors in our estimates of summit elevation change because the magnitude of summit erosion is so small. It is therefore inescapable that, for each range studied, the summit erosion roughly offsets the rock uplift driven by range-scale erosion, so that summit elevations appear to have remained essentially constant (Table 1).

Our analysis suggests that although the contrast between summit and valley erosion has indeed resulted in several hundred meters of geophysical relief change, summit elevations have not significantly increased. This is because the Laramide ranges examined here are narrow relative to the flexural wavelength of the lithosphere (Hetenyi, 1946). In wider ranges, such as the Sierra Nevada or the Himalayas, the reduction in rock uplift due to lithospheric rigidity is less, and the magnitude of erosionally driven summit elevation changes should be greater for erosion of a similar magnitude (e.g., Small and Anderson, 1995).

GLACIAL FEEDBACKS

If summit and ridge elevations have not substantially increased due to erosional unloading, then a positive feedback mechanism between valley-glacier erosion and glacial mass balance, linked by erosionally driven increases in elevation, cannot exist. However, other erosion and mass-balance interactions driven by valley growth, especially valley deepening, may be important. Because lithospheric rigidity limits rock uplift, alpine glacier erosion should lower the spatially averaged elevation of all points within valleys, which we refer to as the mean valley elevation. Changes in mean valley elevation nearly equal changes in the mean elevation of the landscape, because valleys represent ~90% of Pleistocene glaciated regions (discussed above). According to equations 2 and 3 and measured values of $\hat{R}$, the decrease in mean valley elevation associated with geophysical relief production is ~250–300 m, assuming constant valley width. This is a substantial change with respect to alpine glacier mass balance, as it represents ~40% of the equilibrium-line altitude change between the last glacial maximum and today (Porter et al., 1982). As geophysical relief has been produced, this decrease in valley elevation could reduce glacier net mass balance, leading to smaller glaciers and perhaps reduced erosion. However, changes in valley morphology, also resulting from valley growth, could have the opposite effect. As valley depth increases, both topographic shading and aerodynamic entrapment of snow by valley walls will increase, enhancing glacier mass balance.

ONSET OF RELIEF PRODUCTION

We can estimate the onset of geophysical relief production, or valley growth, from our estimates of summit and mean valley erosion rates and the present geophysical relief ($t = \hat{R}/(\dot{E}_V - \dot{E}_S)$). This is a maximum estimate because the calculation is based on the assumption that the initial geophysical relief was negligible. If the long term contrast between valley and summit erosion rates equals the existing contrast (~100 m/m.y.), the onset of valley growth would have occurred roughly 2–3 million years ago. Uncertainty in this estimate is due primarily to poor constraints on the mean valley erosion rate. For example, doubling the long-term mean valley erosion rate (to 200 m/m.y.) lowers the estimate to 1.5 million years ago. Within the uncertainty of our estimate, the onset of geophysical relief production is approximately synchronous with the global cooling event responsible for growth of the Northern Hemisphere continental ice sheet (e.g., Tiedemann et al., 1994). We hypothesize that this valley growth was climatically driven, was synchronous across many Laramide ranges, and was associated with the onset or enhancement of alpine glaciation in these ranges.

CONCLUSIONS

1. Geophysical relief is currently increasing in many Laramide mountain ranges because long-term average valley erosion rates are ~100 m/m.y. faster than those on adjacent summit flats.

2. In Laramide ranges, the geophysical relief, or the average depth of erosion from a smooth surface fit to summits and ridges, is ~300 m. Because Laramide ranges are narrow relative to the flexural wavelength of the lithosphere, maximum rock uplift driven by valley erosion is only 50–100 m. Slow summit erosion, dominated by periglacial processes, has likely offset this minimal rock uplift.

3. Given the mismatch in the long term average rates of valley and summit erosion, the present valleys would be created in 2–3 million years. The inferred onset of relief production at ca. 2–3 Ma may be the result of global cooling and the associated enhancement of alpine glaciation in these mountain ranges.

ACKNOWLEDGMENTS

This work was funded by a grant from the National Aeronautics and Space Administration Surface Topography and Change Program. We thank Doug Burbank and Carol Prentice for helpful reviews. We also thank Greg Dick and Quentin Lindh for help in the field and Max Kaufmann for his aid in the generation of the GIS-based analyses.

REFERENCES CITED

Abbott, L. D., Silver, E. A., Anderson, R. S., Smith, R., Ingle, J. C., King, S. A., Haig, D., Small, E., Galewsky, J., and Sliter, W., 1997, Measurement of tectonic surface uplift rate in a young collisional mountain belt: Nature, v. 385, p. 501–507.

Ahnert, F., 1970, Functional relationships between denudation, relief, and uplift in large mid-latitude drainage basins: American Journal of Science, v. 268, p. 243–263.

England, P., and Molnar, P., 1990, Surface uplift, uplift of rocks, and exhumation of rocks: Geology, v. 18, p. 1173–1177.

Gilchrist, A. R., Summerfield, M. A., and Cockburn, H. A. P., 1994, Landscape dissection, isostatic uplift, and the morphologic development of orogens: Geology, v. 22, p. 963–966.

Hall, M. K., and Chase, C. G., 1989, Uplift, unbuckling, and collapse—Flexural history and isostasy of the Wind River Range and Granite Mountains, Wyoming: Journal of Geophysical Research, v. 94, p. 17581–17593.

Hallet, B., Hunter, L., and Bogen, J., 1996, Rates of erosion and sediment evacuation by glaciers: A review of field data and their implications: Global and Planetary Change, v. 12, p. 213–235.

Hetenyi, M., 1946, Beams on elastic foundation: Ann Arbor, University of Michigan Press, 255 p.

Madole, R. F., Bradley, W. C., and Lowenherz, D. S., 1987, Rocky Mountains, *in* Graf, W. L., ed., Geomorphic systems of North America: Boulder, Colorado, Geological Society of America, Geology of North America, v. 2, p. 211–257.

Molnar, P., and England, P., 1990, Late Cenozoic uplift of mountain ranges and global climate change: Chicken or egg?: Nature, v. 346, p. 29–34.

Montgomery, D. R., 1994, Valley incision and the uplift of mountain peaks: Journal of Geophysical Research, v. 99, p. 13913–13921.

Mitasova, H., and Mitas, L., 1993, Interpolation by regularized spline with tension: I. Theory and implementation: Mathematical Geology, v. 25, p. 641–655.

Porter, S. C., Pierce, K. L., and Hamilton, T. D., 1982, Late Wisconsin mountain glaciation in the western United States, *in* Porter, S. C., ed., Late Quaternary environments of the United States: The late Pleistocene, v. 2, p. 71–111.

Raymo, M. E., and Ruddiman, W. F., 1992, Tectonic forcing of late Cenozoic climate: Nature, v. 359, p. 117–122.

Ruddiman, W. F., and Kutzbach, J. E., 1989, Forcing of late Cenozoic Northern Hemisphere climate by plateau uplift in southern Asia and the American West: Journal of Geophysical Research, v. 94, p. 18409–18427.

Small, E. E., and Anderson, R. S., 1995, Geomorphically driven late Cenozoic rock uplift in the Sierra Nevada, California: Science, v. 270, p. 277–280.

Small, E. E., Anderson, R. S., Repka, J. L., and Finkel, R., 1997, Erosion rates of alpine bedrock summit surfaces deduced from in situ ^{10}Be and ^{26}Al: Earth and Planetary Science Letters, v. 150, p. 413–425.

Small, E. E., Anderson, R. S., and Dick, G. S., 1998, Estimates of regolith production from ^{10}Be and ^{26}Al : Evidence for steady state alpine hillslopes: Geomorphology, (in press).

Tiedemann, R., Sarnthein, M., and Shackleton, N., 1994, Astronomic timescale for the Pliocene Atlantic δ^{18}O and dust flux records of Ocean Drilling Program Site 659: Paleoceanography, v. 9, p. 619–638.

Turcotte, D., and Schubert, G., 1982, Geodynamics: Applications of continuum physics to geological problems: New York, John Wiley and Sons, 450 p.

Manuscript received August 25, 1997
Revised manuscript received November 12, 1997
Manuscript accepted November 21, 1997